arXiv:1304.8095v1 [cond-mat.quant-gas] 30 Apr 2013

LA-UR-13-21407

Experimental realization of Josephson junctions for an Atom SQUID

C. Ryu, A. A. Blinova, P. W. Blackburn, and M. G. Boshier
P-21, Physics Division, Los Alamos National Laboratory, Los Alamos, New Mexico 87545

We report the creation of ideal Josephson junctions in a toroidal dilute gas Bose-Einstein condensate (BEC). The demonstrated configuration of a pair of junctions on a multiply-connected BEC is the cold atom analog of the well-known dc Superconducting Quantum Inteference Device (SQUID). We measure the critical current of the junctions, observe Josephson effects, and find dynamic behavior that is in good agreement with the simple Josephson equations for an ideal tunnel junction with a sinusoidal current-phase relation. The junctions and toroidal trap are created with the Painted Potential, a time-averaged optical dipole potential technique which will allow scaling to more complex BEC circuit geometries than the single Atom-SQUID case reported here. Since rotation plays the same role in the Atom SQUID as magnetic field does in the dc SQUID magnetometer, the device has potential as a compact rotation sensor. It may also be useful for creating macroscopic Schrödinger Cat states.

The dc Superconducting Quantum Interference device (SQUID) [1] was created to study and utilize the quantum interference of currents flowing in parallel through Josephson junctions connected in a superconducting loop. Today, dc SQUIDs, and the more recently-developed rf SQUIDs, are the basis of some of the most sensitive magnetometers [1]. An "Atom SQUID" is an analogous quantum interference device that uses a superfluid dilute gas Bose-Einstein condensate (BEC) [2, 3] flowing through potential barriers in a trap. The superfluid counterpart of the SQUID response to magnetic fields is an analogous response to rotation, which has already been demonstrated in the laboratory with superfluid helium analogs of the SQUID having sensed the rotation of the Earth [4–6]. The Atom SQUID is particularly attractive for rotation sensing and for addressing basic questions in quantum physics because of the advantages of easy detection of BEC atom number and phase, along with the existence of accurate well developed microscopic theories of condensate physics.

An Atom SQUID has two essential ingredients: a multiply-connected geometry trap with quantization of superfluid circulation, and potential barriers (junctions) exhibiting Josephson effects. Like SQUIDs, Atom SQUIDs can have two different types: a "dc Atom SQUID" with two junctions, and an "rf Atom SQUID" with a single junction. Previously, we created a BEC in a toroidal trap and demonstrated quantization of circulation in that system [7]. Here we report the first experimental creation of Josephson junctions in a toroidal trap and the observation of Josephson effects with them. Both the double Josephson junctions and the toroidal trap for a dc Atom SQUID were created with the "Painted Potential" technique [8]. This technique is general and may be used to create arrays of Josephson junctions with complex spatial and temporal variations. To demonstrate Josephson effects, a bias current was imposed by moving the two junctions relative to each other. Compression of atoms was observed when the bias current exceeded the critical current of the junctions, allowing the critical currents to be measured. This advance opens the door to the study of Atom SQUID physics, including the investigation of quantum interference of currents due to rotation and its application to rotation sensing.

Creating an Atom SQUID is a challenge because both the toroidal trap and the Josephson junctions are complex potentials that go beyond conventional magnetic or optical dipole trapping geometries. BECs have been created in toroidal traps using a magnetic trap with a repulsive optical trap at the centre [9], a Laguerre-Gaussian mode of a laser beam [10, 11], and a Painted Potential [7, 8]. Separately, Josephson junctions for BECs have been realized with interference of laser beams [12], a magnetic trap with a repulsive barrier from a laser beam [13], and a radio frequency dressed magnetic trap [14]. Recently [10, 15], a separate laser beam was used to create a barrier for atoms in a toroidal trap, realizing an atom circuit for studying the interesting physics of phase slips [16] in a BEC. That toroidal atom circuit with a single rotating barrier is an atomic analog of a "single junction dc SQUID", a novel configuration which has not been studied in detail in the context of superconductors. The thick (compared to the healing length) and low (50% of the chemical potential) barrier used in that experiment did not form an ideal Josephson junction, and the experiment did not directly demonstrate Josephson effects. In this paper, we report the first experiments showing Josephson effects for a BEC in a multiply-connected geometry. The junctions in the toroidal trap, realized with the Painted Potential technique, are thin and high potential barriers with significant quantum tunneling. As a result they behave as ideal Josephson junctions with a sinusoidal current-phase relation.

The Painted Potential technique [7, 8] realizes complex dynamic potentials for BECs by rapidly moving far-detuned laser beams to create time-averaged optical dipole potentials. Improvements to the setup described in Ref. [8], in particular a new long distance microscope objective (N.A. = 0.4), make the spatial resolution of the Painted Potential (1.5 μm) comparable to the heal-

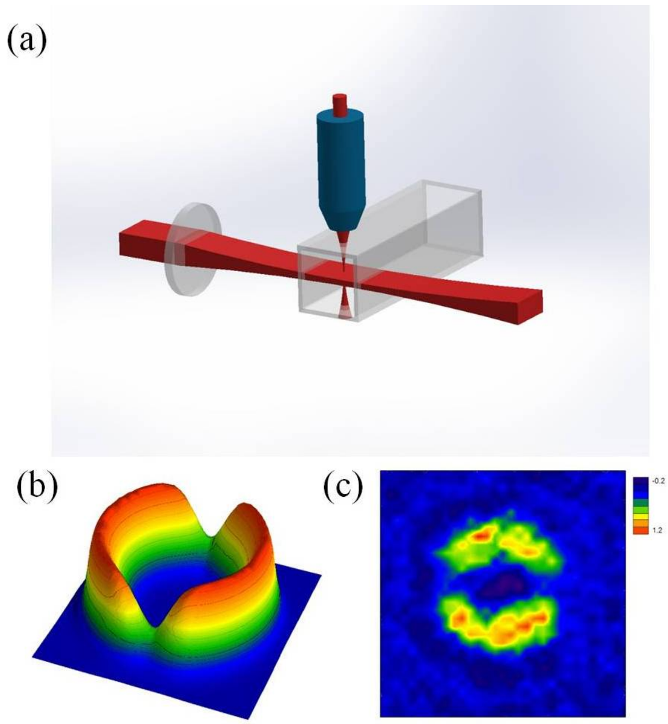

FIG. 1: (a) Schematic of the experimental set up. Arbitrary and dynamic potentials for the BEC are created by the superposition of two red-detuned beams making attractive optical dipole potentials. One beam is a horizontal light sheet, the other is a rapidly moving focused beam which paints the potential. (b) Calculated intensity distribution of $8\,\mu$m diameter painted Atom SQUID potential. (c) *In situ* absorption image of a BEC in the Atom SQUID potential.

ing length of a BEC so that painted potential barriers can exhibit significant tunneling rates. Figure 1(a) is a schematic drawing of the setup. A horizontal scanning beam creates a flat two dimensional (2D) potential for supporting atoms against gravity, while the vertical painting beam creates a complex dynamic potential for a BEC. This high resolution system enables painting of many variations of complex Josephson junctions, including the dc Atom SQUID configuration of double Josephson junctions on a toroidal trap. Figure 1(b) shows the calculated beam intensity distribution for this case where the intensity is lowered in two symmetric locations to create tunneling barriers for a BEC, and Fig. 1(c) shows the *in situ* absorption image of a BEC in this potential. The FWHM (full-width at half-maximum) of the barrier is $2\,\mu$m, which is small enough for a BEC to have a significant tunneling rate (of order a few hundred Hz).

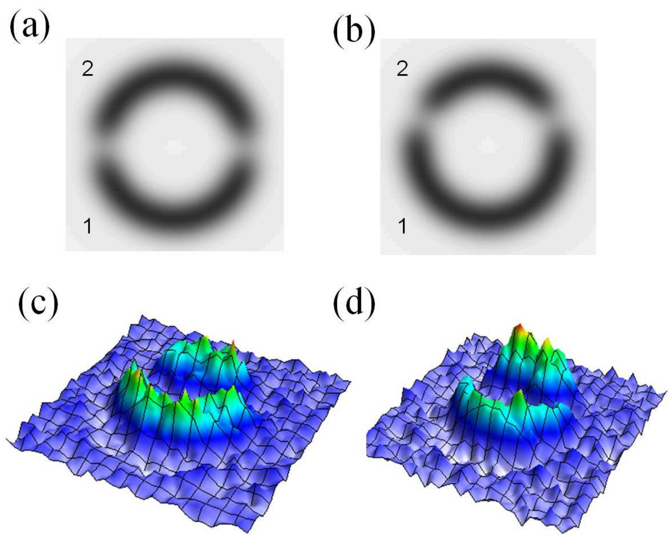

FIG. 2: (a) Initial configuration of Atom SQUID potential. (b) Final potential after the movement of the two Josephson junctions. (c) Image of a BEC where bias current is less than critical current. (d) Image of a BEC where bias current exceeds critical current, showing the BEC compression which occurs when tunneling is not possible.

It is hard to observe Josephson oscillations in this system directly because of their small amplitude. We therefore used the scheme suggested in Ref. [17] to study Josephson effects. In our implementation of this idea, moving the junctions circumferentially towards each other leaves the BEC density unchanged as long as atoms can tunnel through the junctions to maintain the same chemical potential in both sectors of the torus. This phenomenon of a current of atoms flowing without a chemical potential difference is the dc Josephson effect in this system. The current will increase with barrier velocity until the critical current of the Josephson junctions is reached, at which point the system switches to the ac Josephson regime. Here there is an oscillating current of atoms through the barrier, with frequency proportional to the chemical potential difference across the junctions, but no net current across the junctions. Therefore at barrier velocities greater than the speed limit imposed by the critical current, the moving Josephson junctions simply push the atoms, resulting in compression of atoms in one side and expansion in the other. Figure 2(a) and (b) show the initial and final potentials of the Atom SQUID for the movement of Josephson junctions. Figure 2(c) shows the unchanged density distribution of atoms when atoms tunnel through barriers to maintain equilibrium and Fig. 2(d) shows the compressed cloud of atoms in one side when the junctions move too fast for tunneling. This data is the first demonstration of Josephson effects in a toroidal BEC. The rest of the paper discusses the relevant theory and the experimental results in detail.

The simplest theoretical model for the experiment is based on the Josephson equations developed for a BEC [17, 18]. Although our Atom SQUID setup has two junctions, because the two junctions are symmetric and there is no rotation the system can be modeled as two condensates connected by a single junction. Letting N_1, N_2 and ϕ_1, ϕ_2 be the number and phase of atoms in the two sides of the torus, and defining the relative population difference $z = (N_1 - N_2)/(N_1 + N_2)$ and the relative phase difference $\phi = \phi_1 - \phi_2$, the Josephson equations are

$$\dot{z} = I_c \sqrt{1 - z^2} \sin \phi \tag{1}$$

and

$$\dot{\phi} = -\omega_C (z - z_0) - I_c \frac{z}{\sqrt{1 - z^2}} \cos \phi. \tag{2}$$

Here $I_c = 2E_J/\hbar N$ is the critical normalized current of the double junction, where E_J is the Josephson coupling energy [17, 19] and $N = N_1 + N_2$ is the total number of atoms. Also, $\omega_C = E_C/2\hbar N$, where E_C is the capacitance energy [17, 19], and z_0 is the population difference in the equilibrium condition where the chemical potential difference

$$\mu = \mu_1 - \mu_2 = \hbar\omega_C (z - z_0) \tag{3}$$

is zero (μ_1 and μ_2 are the chemical potentials in the two sides of the torus). Equations (1) and (2) determine the evolution of the number and phase differences from given initial conditions. The derivative $\dot{z}$ is a normalized atom current, with maximum value I_c. Changing the equilibrium population difference z_0 creates an effective bias current $\dot{z}_0$. Our experiment follows the proposal by Giovanazzi *et al.* [17] to create $\dot{z}_0$ through the relative movement of Josephson junctions against a BEC. This movement changes the trapping volumes in each side [Fig. 2(a) and (b)] and hence the number difference at equilibrium, which creates the desired bias current. As discussed above, $\dot{z}_0 < I_c$ is the dc Josephson regime in which the chemical potential remains the same in both sides of the torus, while for $\dot{z}_0 > I_c$ (ac Josephson regime) there is no dc current and so the atoms are compressed in one side and expanded in the other.

We now discuss details of the experiment. A BEC of ^{87}Rb atoms was prepared in a potential with trapping frequencies of 300 Hz in the vertical direction of the horizontal trap and 570 Hz along the radial direction of the toroidal trap. The preparation of the BEC starts with the trapping and evaporative cooling of atoms in a quadrupole magnetic trap. ^{87}Rb atoms in the $F = 1$ and $m_F = -1$ state were cooled to $30\,\mu$K and transferred to the combined optical trap. The horizontal trapping beam, with wavelength $\lambda = 1064$ nm and waist $\omega_0 = 11\,\mu$m, was scanned horizontally at 14 kHz over a width of $47\,\mu$m, creating a flat 2D potential for the atoms. The vertical trapping beam, with $\lambda = 830$ nm and $\omega_0 = 1.5\,\mu$m, painted the potential at a scan frequency of 25 kHz, creating here an $8\,\mu$m diameter ring with two intensity minima forming Josephson junctions. Evaporation in the combined optical trap was accomplished by lowering the horizontal trap depth from $40\,\mu$K to $1.1\,\mu$K in 2.5 s while the depth of the vertical painting potential remained fixed at 75 nK. The result was a pure BEC with atom number N set between 1000 and 8000, corresponding to chemical potentials from 29 nK to 58 nK. To prevent excitation of flow of atoms in the BEC creation process, the initial potential had weaker barriers (22 nK). This was sufficient to prevent any rotation of the atoms in the toroidal trap throughout the evaporation process. At the end of the evaporation stage the barrier height was increased to the final value of 44 nK in 100 ms. The two junctions were then moved towards each other at a rotation frequency f for each junction, which gives rise to a bias current $\dot{z}_0 = 4f$. To prevent plasma oscillations and to establish the bias current adiabatically, the barriers were accelerated at constant rate to the desired constant velocity. The total compression angle for each junction was $\pi/8$ and the compression angle after the acceleration stage was 0.06π. Following the movement of the Josephson junctions, the BEC was imaged by absorption *in situ*. The clear change seen in the final density distribution between the dc Josephson [Fig. 2(c)] and ac Josephson [Fig. 2(d)] regimes as the bias current increases can identify the critical current accurately.

Predicted critical currents were obtained from Josephson coupling energies computed by applying the improved two mode model of Ananikian and Bergeman [19] to accurate numerical wavefunctions generated through direct minimization of the appropriate Gross-Pitaevskii energy functional. The results are plotted in Fig. 3 for three different potential depths, showing that the critical current may be varied substantially over the range of atom numbers accessible to the experiment. Figure 3 also illustrates the dependence of critical current on potential depth, which arises because the critical current depends on tunneling (the Josephson coupling energy E_J) which in turn depends on the barrier height, which is here a fixed fraction of the trap depth.

Data was collected by fixing the bias current and varying the atom number. It is straightforward to determine the total number of atoms N and the normalized number difference z from the absorption images. Figure 4(a)-(c) shows three data sets corresponding to barrier rotation frequencies of $1\,\mathrm{s}^{-1}$, $2\,\mathrm{s}^{-1}$, and $4\,\mathrm{s}^{-1}$. The sharp transition from dc to ac Josephson regimes is seen as the sudden change of normalized population difference z as the atom number N decreases. The transition point, corresponding to the atom number where the bias current is equal to the critical current, shifts to higher N as the bias current increases, in accordance with Fig. 3. To make a quantitative comparison with theory we find the best least-squares fit to each data set of a numerical integration of the Josephson equations (1) and (2). Each fit had three free parameters: the potential depth, and the initial and final values of the normalized population difference z. These parameters are determined by the fit because slight deviations of the initial and final population differences from the values predicted by geometry result from imperfections in the toroidal potential, and drifts of a

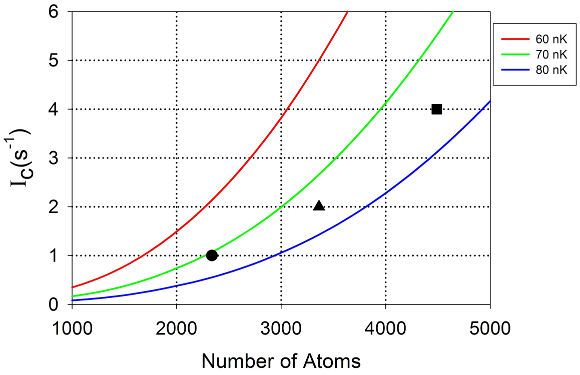

FIG. 3: Solid lines show computed critical current as a function of BEC atom number for three different toroidal trap depths. Points show the measured critical atom number determined by fitting a Josephson equation model to data sets for the three currents employed in the experiment (see text). Critical currents and fitted trap depth are respectively: $1\,\mathrm{s}^{-1}$ and $71\,\mathrm{nK}$ (circle), $2\,\mathrm{s}^{-1}$ and $74.5\,\mathrm{nK}$ (triangle), $4\,\mathrm{s}^{-1}$ and $75.6\,\mathrm{nK}$ (square).

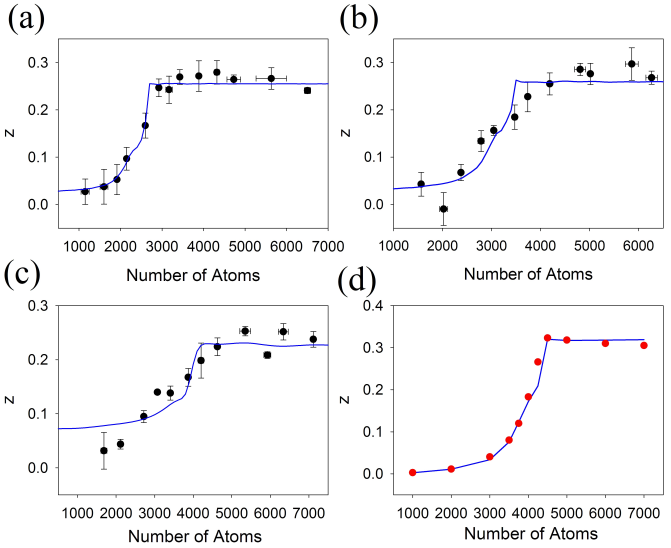

FIG. 4: (a) - (c): Measurement of critical currents. Each data point is the mean of several measurements of the final normalized population difference z, with the error bar being the standard error of the mean. The blue curves show the best fit numerical integration of the Josephson equations. For the three data sets, the junction rotation frequency f, corresponding bias current $\dot{z}$, and duration of junction movement T are: (a) $f = 0.25\,\mathrm{Hz}$, $\dot{z} = 1\,\mathrm{s}^{-1}$, $T = 370\,\mathrm{ms}$. (b) $f = 0.5\,\mathrm{Hz}$, $\dot{z} = 2\,\mathrm{s}^{-1}$, $T = 185\,\mathrm{ms}$. (c) $f = 1\,\mathrm{Hz}$, $\dot{z} = 4\,\mathrm{s}^{-1}$, $T = 92.5\,\mathrm{ms}$. (d) Predicted final value of normalized population difference z for $f = 1\,\mathrm{Hz}$ (bias current $\dot{z} = 4\,\mathrm{s}^{-1}$) in a flat trap computed using numerical integration of the Josephson equations (blue line) and the 3D Gross-Pitaveskii equation (red disks).

few μm in the relative waist positions of the horizontal and vertical trapping beams can introduce small variations in trap depth between data sets. The fits, shown as the blue curves in Fig. 4, are in generally good agreement with the data. The potential depths obtained from the fits (71 nk, 74.5 nk, and 75.6 nK respectively) are within the range expected from our estimate of possible relative drift of the waists of the trapping beams. The critical atom numbers determined by the fit for each rotation frequency are shown on Fig. 3. Their consistency with the theory predictions (for the trap depths determined by the fits) illustrates the agreement between experiment and theory seen in Fig. 4(a)-(c).

The model based on the Josephson equations (1) and (2) is simple, neglecting, for example, changes in the coupling and capacitive parameters as the barriers move and also any consequences of excitations in the condensate. To quantify the impact of such effects we performed full three dimensional (3D) dynamic simulations for parameters appropriate to our experiment using the Gross-Pitaevskii equation (GPE). The results, shown in Fig. 4(d), are in excellent agreement with the predictions of the simple Josephson equations. This result confirms the validity of the Josephson equations for describing our experiments, and it shows that the Atom SQUID can be well understood from microscopic theories without relying on phenomenological models. This finding may be beneficial in the design and interpretation of future experiments with Atom SQUIDs. Further, the agreement between the GPE results, the data, and the Josephson equations confirms that the experiment realizes ideal Josephson tunnel junctions obeying the sinusoidal current-phase relation given by Eq. (1). It follows that the system reported here is exactly analogous to the ideal dc SQUID, and so superfluid analogs of the phenomena seen in that device should also be observable in the device described here.

In summary, we have demonstrated Josephson effects in a toroidal trap for the first time, by showing the transition between the dc and ac Josephson regimes and by measuring the critical current of the junctions. The experimental data for our dc SQUID geometry is in good agreement with the predictions of the Josephson equations. Looking to the future, the quantization of circulation in the toroidal trap geometry will lead to quantum interference of currents in the dc Atom SQUID as a function of rotation rate. The interference can be demonstrated by measuring the shift of critical current with trap rotation rate (rotating the junctions is straightforward with the Painted Potential technique), enabling the use of Atom SQUIDs for rotation sensing. The Atom SQUID interaction region can be compact, so it will be interesting to compare its rotation-sensing performance with the current state of the art, the large area atom optics-based gyroscope [20]. Another future direction, relevant to both sensing and basic quantum physics, is applying the technology demonstrated here to recent proposals [21–26] to create Schrödinger Cat states of different flow states in an Atom SQUID. These states are analogous to the Schrödinger Cat states of different flux states demonstrated in SQUIDS [27, 28], and now used as qubits in quantum information processors [29]. There has been considerable discussion regarding the true number of entangled particles in these systems [30, 31] and so it would be intriguing to duplicate the experiment with a BEC where, in contrast to the SQUID, the microscopic physics is almost completely understood.

We gratefully acknowledge inspiring conversations with Eddy Timmermans and Dima Mozyrsky. This work was supported by the U.S. Department of Energy through the LANL/LDRD program.

[1] J. Clarke, and A. I. Braginski, *The SQUID Handbook* (Wiley-VCH, Weinheim, 2004).

[2] M. H. Anderson, J. R. Ensher, M. R. Matthews, C. E. Wieman, and E. A. Cornell, Science **269**, 198 (1995).

[3] K. B. Davis, M. O. Mewes, M. R. Andrews, N. J. van Druten, D. S. Durfee, D. M. Kurn, and W. Ketterle, Phys. Rev. Lett. **75**, 3969 (1995).

[4] K. Schwab, R. Bruckner, and R. E. Packard, Nature **386**, 585 (1997).

[5] O. Avenel, P. Hakonen, and E. Varoquaux, Phys. Rev. Lett. **78**, 3602 (1997).

[6] Y. Sato, and R. E. Packard, Rep. Prog. Phys. **75**, 016401 (2012).

[7] C. Ryu, K. C. Henderson, and M. G. Boshier, to be published (2013).

[8] K. Henderson, C. Ryu, C. MacCormick, and M. G. Boshier, New J. Phys. **11**, 043030 (2009).

[9] C. Ryu, M. F. Andersen, P. Clade, V. Natarajan, K. Helmerson, and W. D. Phillips, Phys. Rev. Lett. **99**, 260401 (2007).

[10] A. Ramanathan, K. C. Wright, S. R. Muniz, M. Zelan, W. T. Hill, C. J. Lobb, K. Helmerson, W. D. Phillips, and G. K. Campbell, Phys. Rev. Lett. **106**, 130401 (2011).

[11] S. Moulder, S. Beattie, R. P. Smith, N. Tammuz, and Z. Hadzibabic, Phys. Rev. A **86**, 013629 (2012).

[12] M. Albiez, R. Gati, J. Folling, S. Hunsmann, M. Cristiani, and M. K. Oberthaler, Phys. Rev. Lett. **95**, 010402 (2005).

[13] S. Levy, E. Lahoud, I. Shomroni, and J. Steinhauer, Nature **449**, 579 (2007).

[14] L. J. LeBlanc, A. B. Bardon, J. McKeever, M. H. T. Extavour, D. Jervis, J. H. Thywissen, F. Piazza, and A. Smerzi, Phys. Rev. Lett. **106**, 025302 (2011).

[15] K. C. Wright, R. B. Blakestad, C. J. Lobb, W. D. Phillips, and G. K. Campbell, Phys. Rev. Lett. **110**, 025302 (2013).

[16] E. Hoskinson, Y. Sato, I. Hahn, and R. E. Packard, Nat Phys **2**, 23 (2006).

[17] S. Giovanazzi, A. Smerzi, and S. Fantoni, Phys. Rev. Lett. **84**, 4521 (2000).

[18] S. Raghavan, A. Smerzi, S. Fantoni, and S. R. Shenoy, Phys. Rev. A **59**, 620 (1999).

[19] D. Ananikian, and T. Bergeman, Phys. Rev. A **73**, 013604 (2006).

[20] T. L. Gustavson, P. Bouyer, and M. A. Kasevich, Phys. Rev. Lett. **78**, 2046 (1997).

[21] A. Nunnenkamp, A. M. Rey, and K. Burnett, Phys. Rev. A **77**, 023622 (2008).

[22] D. W. Hallwood, and J. Brand, Phys. Rev. A **84**, 043620 (2011).

[23] C. Schenke, A. Minguzzi, and F. W. J. Hekking, Phys. Rev. A **84**, 053636 (2011).

[24] D. Solenov, and D. Mozyrsky, Phys. Rev. Lett. **104**, 150405 (2010).

[25] D. Solenov, and D. Mozyrsky, Phys. Rev. A **82**, 061601 (2010).

[26] D. Solenov, and D. Mozyrsky, J. Comput. Theor. Nanosci. **8**, 481 (2011).

[27] C. H. van der Wal, A. C. J. ter Haar, F. K. Wilhelm, R. N. Schouten, C. J. P. M. Harmans, T. P. Orlando, S. Lloyd, and J. E. Mooij, Science **290**, 773 (2000).

[28] J. R. Friedman, V. Patel, W. Chen, S. K. Tolpygo, and J. E. Lukens, Nature **406**, 43 (2000).

[29] J. Clarke, and F. K. Wilhelm, Nature **453**, 1031 (2008).

[30] F. Marquardt, B. Abel, and J. von Delft, Phys. Rev. A **78**, 012109 (2008).

[31] J. I. Korsbakken, F. K. Wilhelm, and K. B. Whaley, Europhys. Lett. **89**, 30003 (2010).